Supporting Information

Vapor-fed solar hydrogen production exceeding 15% efficiency using earth abundant catalysts and anion exchange membrane

Gino Heremans,[a] Christos Trompoukis,[ab] Nick Daems,[a] Tom Bosserez,[a] Ivo Vankelecom,[a] Johan A. Martens[a] and Jan Rongé[a]*

[a]Centre for Surface Chemistry and Catalysis, KU Leuven, Celestijnenlaan 200F, B-3001 Heverlee, Belgium

[b]Department of Information Technology, Photonics Research Group, Ghent University, Technologiepark Zwijnaarde 15, B-9000 Ghent, Belgium

* **Corresponding author**
E-mail: jan.ronge@kuleuven.be

Experimental methods

PVA synthesis: The PVA membranes were made by solution casting as described by Zeng *et al.*[1] A 5 wt% PVA polymer solution was prepared by dissolving 1.05 g of PVA (99%, MW 85.000 – 124.000, Sigma-Aldrich) in 20 g distilled water, which was stirred at 90 °C until a homogeneous solution was obtained. Afterwards, the temperature was decreased to 40 °C and 5 wt% glutaraldehyde (25 wt% in water, Acros Organics) was added dropwise into the solution acting as a crosslinker, and several drops of 1 M NaOH were added as catalyst. After stirring for 2 h and degassing in a vacuum oven for 15 min, the viscous mixture was cast into a clean Teflon petri dish and dried in an oven at 60 °C for 24 h. The thickness of the membranes was measured with scanning electron microscopy (Nova NanoSEM 450, FEI) and amounted to *ca.* 254 ± 32 µm.

Electrode preparation: Earth abundant NiFe and NiMo electrocatalysts were electrodeposited on pieces of carbon paper (TGP-H-030 Toray carbon paper, Fuel Cell Earth). A conducting wire (Conrad, 0.14 mm^2) was attached on the surface of the substrate using silver paint (RS

Components) and the contact was covered with epoxy resin (Loctite M-121MP Hysol, Henkel). Before electrodepositon, the carbon paper was cleaned with ethanol and acetone and dried for 60 minutes at 60 °C. The deposition conditions were based on literature and are summarized in Table S1.[2–4] Each electrodeposition was carried out in a two-electrode cell with a stirred volume of 100 mL. During electrodeposition, intensive stirring of the electrolyte bath was applied with a magnetic bead to prevent mass diffusion limitations. After deposition, the electrodes were rinsed repeatedly with MilliQ water (18.2 MΩ.cm), air-dried and stored in sample boxes in the dark at room temperature.

Materials for electrodeposition of NiMo and NiFe: Nickel sulfate hexahydrate (97%) and ferrous sulfate heptahydrate (99%) were obtained from Honeywell. Ferric chloride hexahydrate (99%) and nickel chloride (99.9%) were obtained from Sigma-Aldrich. Sodium molybdate dihydrate (99.5%) was obtained from VWR International. Ferrous chloride tetrahydrate (99%) and boric acid (99.99%) was obtained from Acros organics. Sodium citrate dihydrate (99%)

Table S1. Electrochemical conditions and composition of the electrolyte baths for the electrodeposition of NiMo and NiFe electrodes.

NiMo	**NiFe**
Cathodic deposition at -160 mA/cm² for 1200 s	Cathodic deposition at -50 mA/cm² for 680 s
79 g/L $NiSO_4 \cdot 6H_2O$	120.6 g/L $NiSO_4 \cdot 6H_2O$
48 g/L $Na_2MoO_4 \cdot 2H_2O$	3.252 g/L $NiCl_2 \cdot 6H_2O$
88 g/L $Na_3C_6H_5O_7 \cdot 2H_2O$	172.944 g/L $FeSO_4 \cdot 7H_2O$
Excess NH_4OH to pH 10.5	3.625 g/L $FeCl_2 \cdot 4H_2O$
	2.825 g/L H_3BO_3
	Excess H_2SO_4 to pH 3

Electrode characterization: Electrocatalytic activity measurements were performed in a one-compartment electrochemical cell with volume of approximately 200 mL. A platinum ring and a Hg/HgO (20 wt% NaOH) electrode (RE-61AP, Bio-logic) served as counter and reference electrode, respectively. Current-voltage curves were recorded at ambient temperature using a

VersaSTAT 4 potentiostat (Princeton Applied Research). To investigate the catalyst activity, cyclic voltammetry measurements were performed. Scan rate was set at 10 mV/s and H_2 or O_2 was purged through 1 M KOH electrolyte for respectively the hydrogen or oxygen evolution reactions prior to measurements to saturate the solution. Reported data were corrected for the uncompensated resistance (R_u) and current densities were normalized to the single-side geometric surface area. R_u was determined by performing potentiostatic impedance spectroscopy at open circuit potential and in a frequency region between 100 Hz and 1 MHz. R_u was extracted from the data by determining the minimum of the real part of the impedance in the high frequency region where phase angle was zero. For the experiment shown in Fig. 2 of the manuscript, R_u was 1.06 Ω for the NiMo sample and 0.82 Ω for the NiFe sample. Geometric areas were determined by taking a photograph of the electrode and using the software ImageJ to calculate the area. The measured potentials were corrected for ohmic losses and referenced to the reversible hydrogen electrode (RHE).

Membrane electrode assembly preparation: An electrolysis device was built with the in-house prepared PVA membrane. Before assembling, the membrane was swollen with KOH by immersing it 24 hours in 4 M KOH. After removing it from the bath, excess KOH on the surface was removed by rinsing multiple times with MilliQ water, followed by blotting to remove liquid water droplets. The membrane electrode assembly was prepared with 4 cm^2 active area by assembling the membrane between NiFe and NiMo coated carbon papers. In this device, carbon paper acted as gas diffusion layer and catalyst support. The membrane electrode assembly was compressed by hand tightening between two graphite plates with serpentine gas flow channels and sealed with gaskets to construct the electrolysis device. Gold-coated end plates were used for making electrical contact.

Electrolysis device characterization: Cyclic voltammetry measurements were performed to evaluate the performance of the device. Before each measurement, the electrolysis device was

flushed with nitrogen gas at a relative humidity of 95% for at least 12 hours. The relative humidity was chosen by mixing water-saturated nitrogen gas with dry nitrogen gas using mass flow controllers. 200 mL/min saturated N_2 was mixed with 10 and 35 mL/min to reach non-condensing gas streams at 95% and 85% relative humidity, respectively. A moisture sensor was placed at the compartment outlets to measure the relative humidity of the output gas streams. No correction was made for resistive losses, in order to show the true performance of this device. Stability of the device was verified with chronopotentiometric measurements at 10 mA/cm². The resistance was measured with electrochemical impedance spectroscopy, which was performed at open circuit potential and at 10 mA/cm² from 1 Mhz to 100 Hz. Resistances were found in the high frequency region where the imaginary impedance was zero. The polarization curves were not corrected for IR losses. The compositions of the outlet gas streams of the anode and cathode compartments were characterized with a mass spectrometer (Hiden Analytical, Warrington, UK). Calibration with nitrogen, oxygen and hydrogen mixtures was performed using mass flow controllers to determine sensitivity factors of the detector prior to quantifying the gas composition. During measurements, inlet flow rates were precisely controlled by mass flow controllers so the relative mass spectrometry signals could be translated into absolute amounts of hydrogen and oxygen. A baseline was determined by linear interpolation of the data points before and after the experiment.

PV module fabrication, characterization and electric coupling: Five solar cells (KXOB22-12X1F, IXYS) were soldered with copper wires at both ends. All solar cells were taped on a Teflon holder, which was clamped at a precise location. Each of the ten solar cell terminals could be connected individually in order to select one, two, three, four or five cells to be connected in series. In this work, three and four solar cells were put in series by connecting the respective copper wires with crocodile clamps. A Xe lamp (Oriel 66984, Newport) with IR and AM 1.5 filters was used to simulate 1 sun illumination. Cyclic voltammetry measurements

were performed at 10 mV/s with a potentiostat (PGSTAT204, Metrohm Autolab) to analyze the iV characteristics of the PV module. The position of the PV module was fixed at a calibrated distance to obtain 1 sun illumination intensity. Electric coupling of the PV module with the electrolysis device was performed with crocodile clamps. The potentiostat was connected in series with the solar hydrogen generator to measure the overall performance with a chronoamperometric measurement under short circuit conditions (zero applied voltage).

Supplementary figures

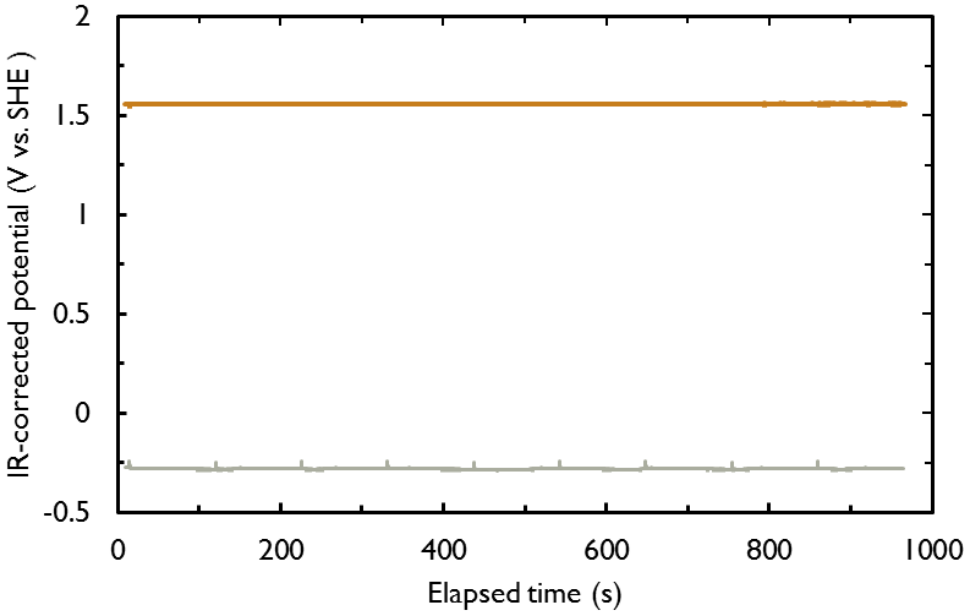

Figure S1. Stability measurement of electrodeposited NiMo (gray) and NiFe (orange) supported on Toray paper. A chronopotentiometric measurement was performed over 900 seconds at respectively -35.4 and 41.6 mA/cm². Every 100 seconds an electrochemical impedance measurement was performed to measure the resistance of the catalyst sample, which remained constant at 0.53 and 0.87 Ω for the NiMo and NiFe catalysts, respectively. Both catalysts remained stable over the duration of the measurement.

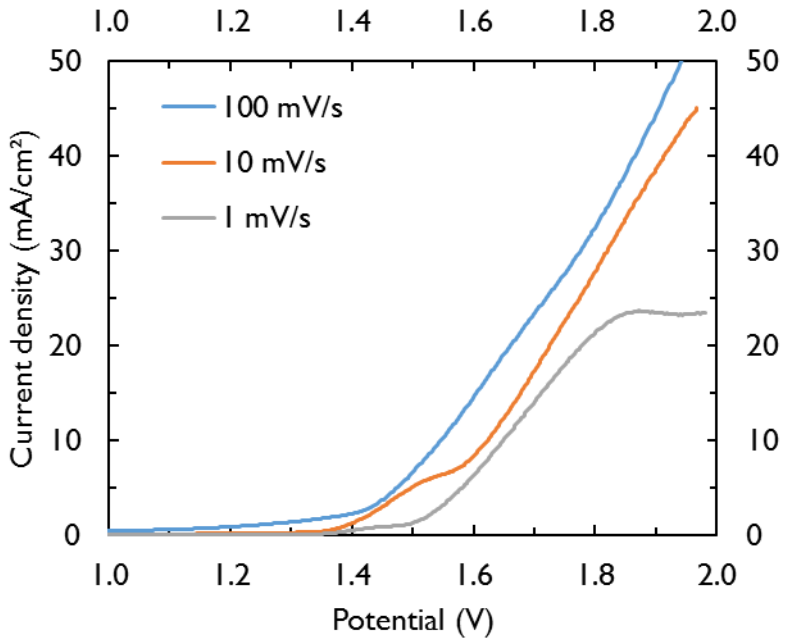

Figure S2. Effect of scan rate on polarization curves of the vapor-fed electrolysis device operated at room temperature in 2-electrode configuration. At high scan rates, the redox wave attributed to nickel oxidation ($Ni(OH)_2$ → NiOOH) becomes clearly visible. At low scan rates, a saturation current density of *ca.* 23 mA/cm^2 can be observed, tentatively attributed to mass transfer limitation of water vapor.

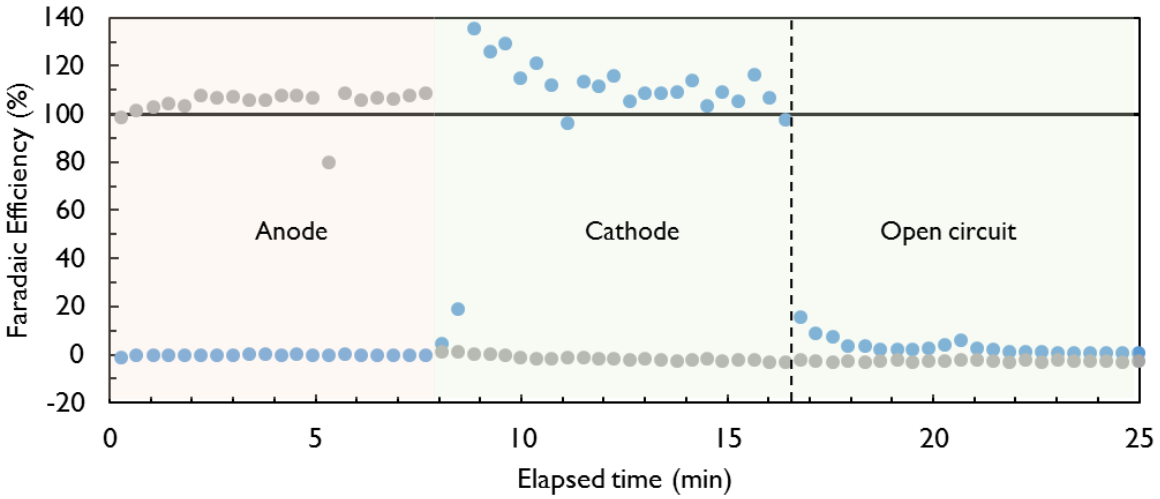

Figure S3. Outlet gas analysis with a mass spectrometer of the electrolysis device operated at 10 mA/cm². The Faradaic efficiencies of hydrogen (blue) and oxygen (grey) gas were calculated for each compartment (anode = red, cathode = green). The average Faradaic efficiency recorded at the anode and at the cathode was 108% and 103%, respectively. The theoretical Faradaic efficiency of 100% is indicated with a black line. A dotted line indicates a transition from constant current electrolysis to open circuit.

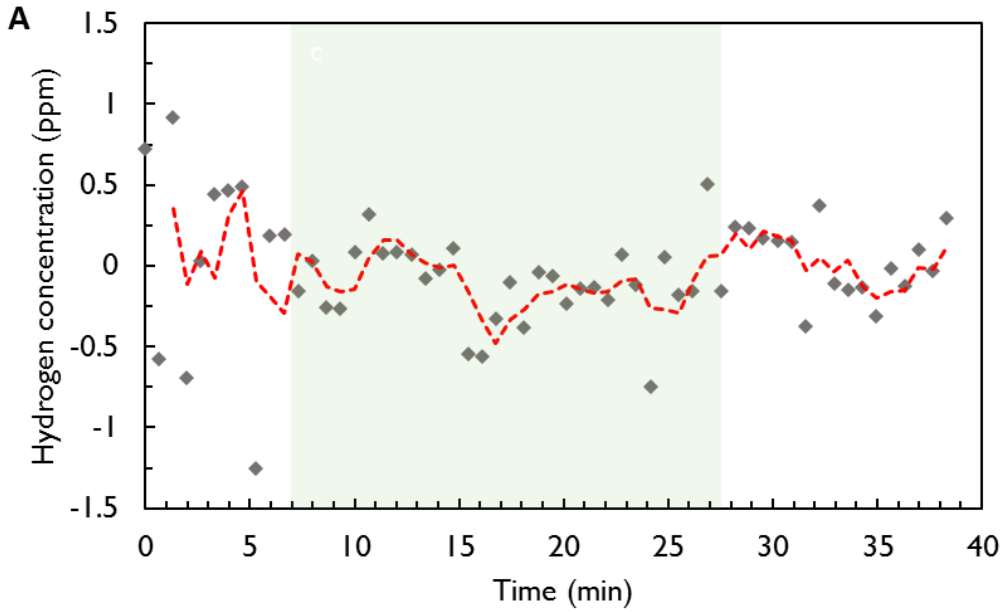

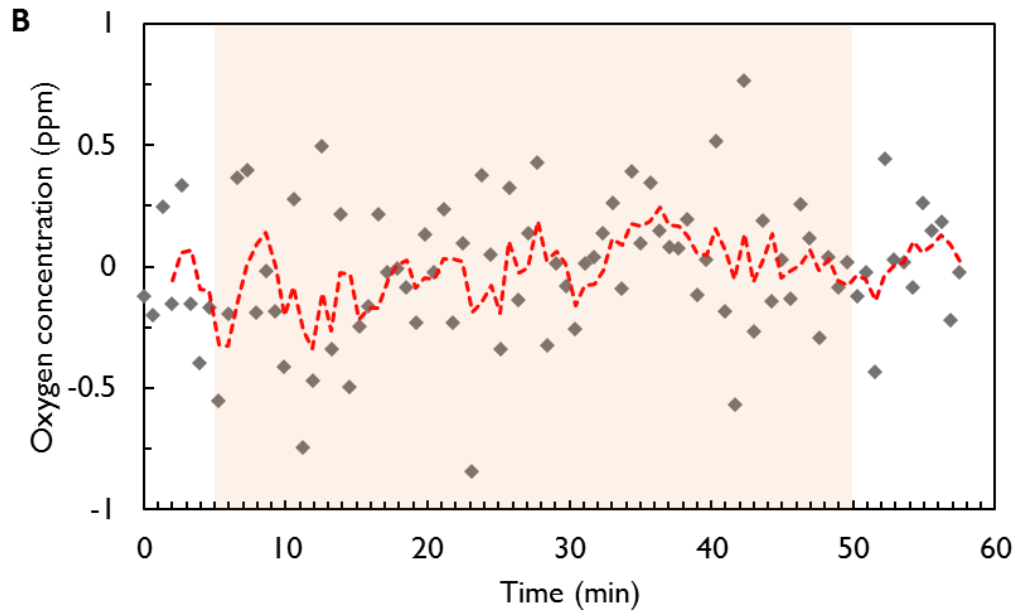

Fig. S4. Determination of gas cross-over using mass spectrometry during open circuit. The outlet gas of one compartment was monitored while the second compartment was fed with nitrogen or the gas of interest. (A) Hydrogen concentration detected at the anode when the cathode was fed with pure hydrogen and the anode was fed with pure nitrogen. The green rectangle indicates when cathode was fed with hydrogen. (B) Oxygen concentration detected at the cathode when the anode was fed with pure oxygen and the anode was fed with pure nitrogen. The red rectangle indicates when anode was fed with oxygen. No cross-over was observed. Detection limits are estimated at 1 ppm hydrogen and 0.5 ppm oxygen, resulting in estimated permeabilities of less than $1.5 \cdot 10^{16}$ mol Pa^{-1} cm^{-1} s^{-1} for hydrogen and less than $7.0 \cdot 10^{17}$ mol Pa^{-1} cm^{-1} s^{-1} for oxygen.

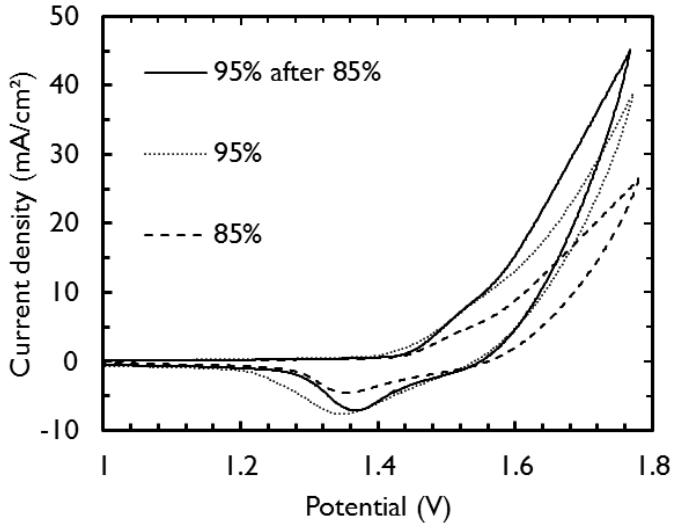

Figure S5. Polarization curves of the electrolysis device under different humidity conditions. Cyclic voltammetry measurements were performed in two-electrode mode at a scan rate of 0.1 V/s and at room temperature. A nitrogen gas flow of 95% or 85% RH was flown through each electrode compartment. After retreatment with 95% relative humidity nitrogen gas, a regeneration of the performance was observed.

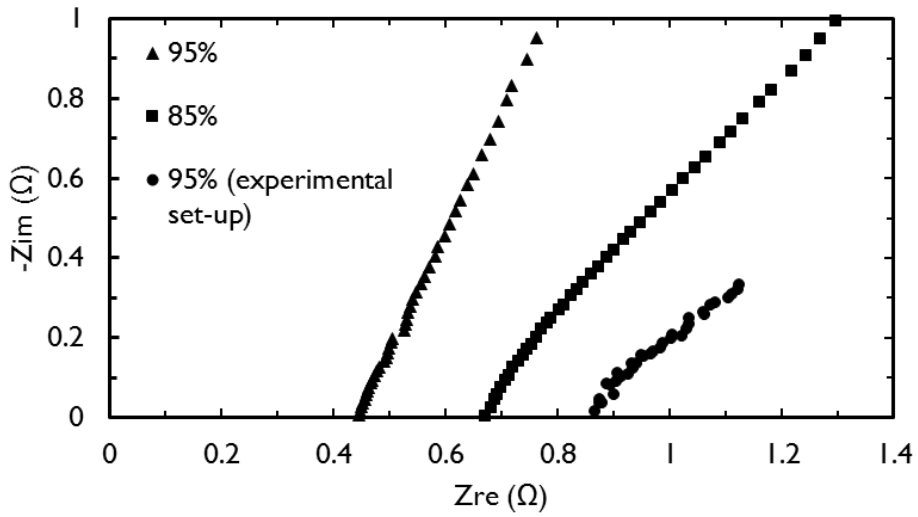

Figure S6. Nyquist impedance plots for the vapor-fed electrolysis device conditioned with nitrogen gas at 95% RH (triangles and circles) and 85% RH (squares). The electrochemical impedance measurements were performed at open circuit potential from 1 Mhz to 100 Hz. Characterization of the stand-alone electrolysis device was performed with long electric wires, which increased the resistance to 0.87 Ohm (circles). For integrated solar hydrogen generation, solar cells were directly connected to the electrolyzer. In this configuration, resistance of the electrolyzer was only 0.44 Ohm (triangles) and can be attributed mainly to membrane resistance. At an average membrane thickness of 254 μm, the membrane conductivity was estimated at 14.4 mS/cm.

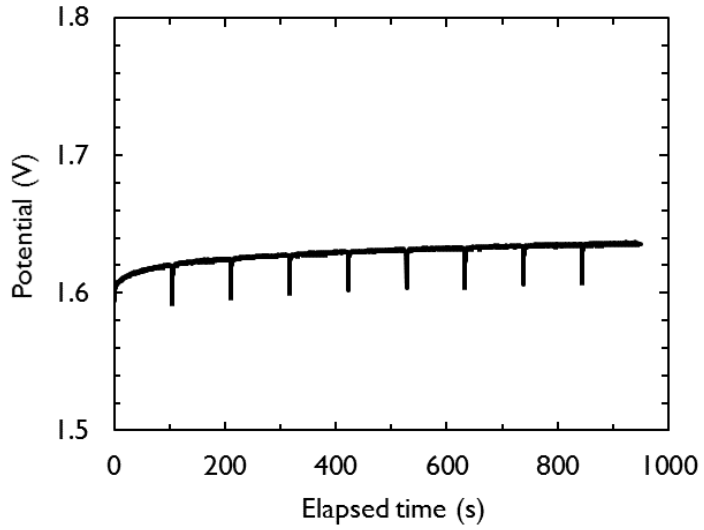

Figure S7. Stability measurement of the vapor-fed electrolysis device. A chronopotentiometric measurement at 10 mA/cm² was performed over 900 seconds. Every 100 seconds an electrochemical impedance measurement was performed to measure the resistance of the electrolysis device. The operating potential increased from *ca.* 1.6 V to 1.635 V. The ohmic losses remained constant at 32 mV during the whole measurement.

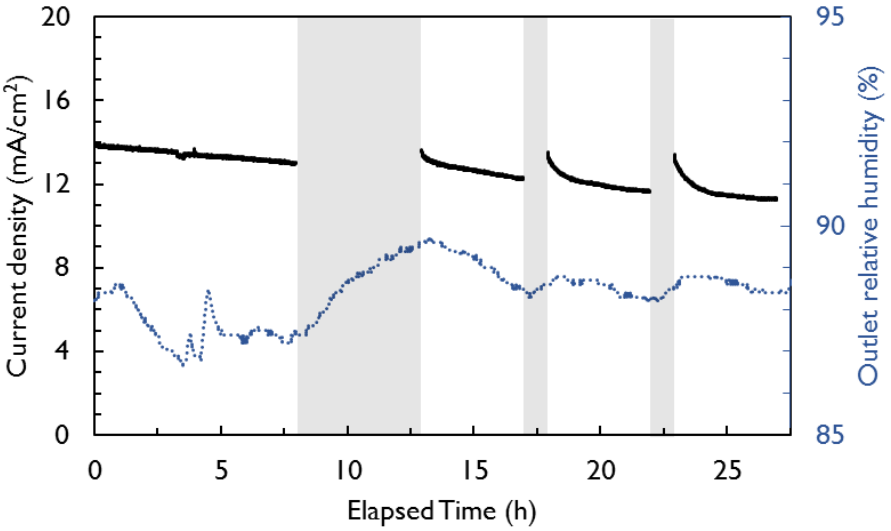

Figure S8. Long stability test of the vapor-fed solar hydrogen generator. A chronoamperometric measurement was performed at short circuit (black trace) during 8 h of illumination. Following a dark period of 5 h, three more illumination periods of 4 h were performed with 1 h dark intervals. The dark periods are indicated by grey shaded areas. During the experiment, the relative humidity was monitored at the cathode outlet (blue dotted line). The measurement was performed with a freshly prepared membrane electrode assembly after *ca.* 2 h of initial testing. The operating potential increased with 240 mV from the start of the measurement to the end. The ohmic losses through the membrane only slightly increased from 15 mV to 16 mV.

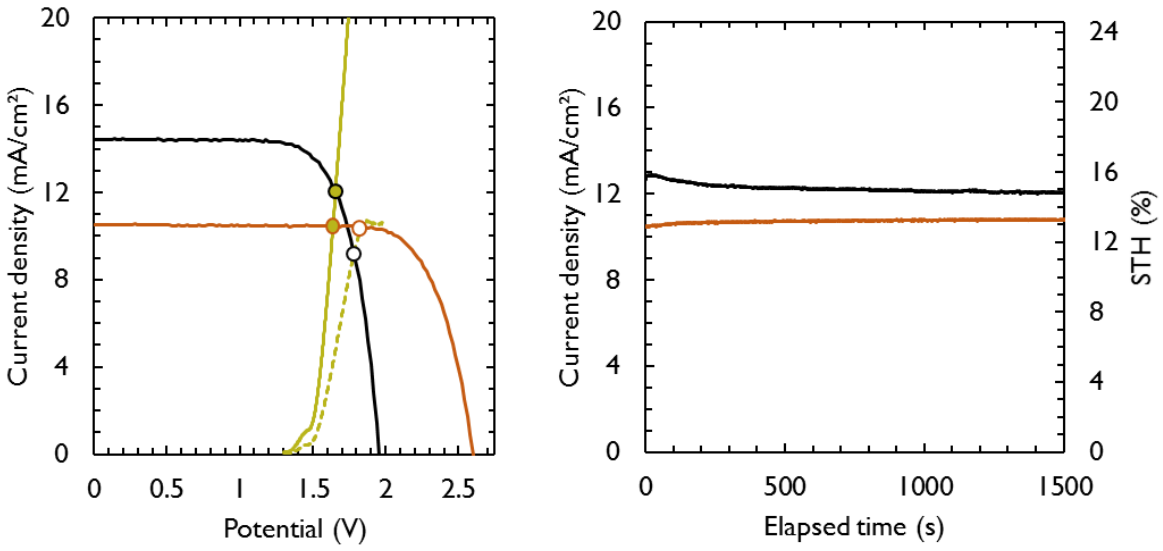

Figure S9. Matching of the vapor-fed electrolysis device with the solar module. (a) Polarization curves of PV modules with three (black) or four (orange) solar cells in series, and the vapor-fed electrolysis device operated at room temperature with current concentration of 0.89 (olive) or 2.50 (dotted olive). At 0.89 current concentration, the highest STH efficiency is achieved with three series-connected solar cells (STH efficiency of 15 %). However, with four series-connected solar cells a nearly three times higher current concentration (three times smaller electrolysis area) is possible without notable performance loss compared to a current concentration of 0.89 (STH efficiency of 12.8%). (b) Chronoamperometric measurement at short circuit over 1500 seconds of the integrated solar hydrogen generator with 3 (black) or 4 (orange) solar cells in series, with current concentration of 0.89 and 1.18, respectively. The average STH efficiency was 15.1% (3 cells) and 13.2% (4 cells). The active area of the solar modules was used to calculate the current densities of all curves.

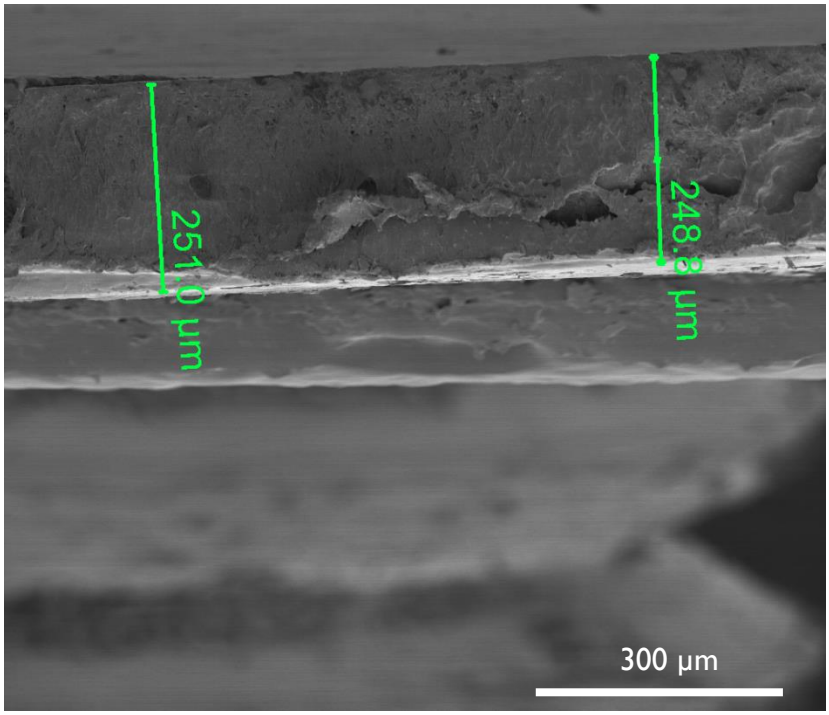

Figure S10. Scanning electron microscope image of a cross section of poly(vinyl alcohol) anion exchange membrane. The membrane was tilted with a screw and fixed with carbon tape. The average membrane thickness amounted to 254 ± 32 µm over several images.

References

1 L. Zeng, T. S. Zhao and Y. S. Li, Int. J. Hydrogen Energy, 2012, **37**, 18425–18432.

2 R. Solmaz and G. Kardas, Electrochim. Acta, 2009, **54**, 3726–3734.

3 C. C. L. McCrory, S. Jung, I. M. Ferrer, S. Chatman, J. C. Peters and T. F. Jaramillo, J. Am. Chem. Soc., 2015, **137**, 4347–4357.

4 E. Navarro-Flores, Z. Chong and S. Omanovic, J. Mol. Catal. A Chem., 2005, **226**, 179–197.